



HAL
open science

Structure of a two-dimensional crystal in a Langmuir monolayer : grazing incidence X-ray diffraction and macroscopic properties

C. Flament, F. Gallet, F. Graner, M. Goldmann, I. Peterson, A. Renault

► To cite this version:

C. Flament, F. Gallet, F. Graner, M. Goldmann, I. Peterson, et al.. Structure of a two-dimensional crystal in a Langmuir monolayer : grazing incidence X-ray diffraction and macroscopic properties. Journal de Physique II, 1994, 4 (6), pp.1021-1032. 10.1051/jp2:1994181 . jpa-00248011

HAL Id: jpa-00248011

<https://hal.science/jpa-00248011>

Submitted on 4 Feb 2008

HAL is a multi-disciplinary open access archive for the deposit and dissemination of scientific research documents, whether they are published or not. The documents may come from teaching and research institutions in France or abroad, or from public or private research centers.

L'archive ouverte pluridisciplinaire **HAL**, est destinée au dépôt et à la diffusion de documents scientifiques de niveau recherche, publiés ou non, émanant des établissements d'enseignement et de recherche français ou étrangers, des laboratoires publics ou privés.

Classification
Physics Abstracts
68.10 — 68.42

Structure of a two-dimensional crystal in a Langmuir monolayer : grazing incidence X-ray diffraction and macroscopic properties

C. Flament ⁽¹⁾, F. Gallet ⁽¹⁾, F. Graner ⁽¹⁾, M. Goldmann ⁽²⁾, I. Peterson ^(2, *) and A. Renault ⁽³⁾

⁽¹⁾ Laboratoire de Physique Statistique de l'ENS (**), 24 rue Lhomond, 75231 Paris Cedex 05, France

⁽²⁾ Laboratoire de Physique des Surfaces et Interfaces, Institut Curie, 11 rue P. et M. Curie, 75231 Paris Cedex 05, France

⁽³⁾ Laboratoire de Spectrométrie Physique, B.P. 87, 38042 St Martin d'Hères Cedex, France

(Received 10 December 1993, received in final form 17 February 1994, accepted 23 February 1994)

Résumé. — Une monocouche de Langmuir, composée d'acide NBD-stéarique fluorescent pur, déposée à la surface libre de l'eau, est analysée par diffraction de rayons X sous incidence rasante. On détecte plusieurs pics étroits et intenses dans la phase solide, aux mêmes vecteurs d'onde que les pics les plus brillants précédemment observés par diffraction électronique, pour une monocouche transférée sur un substrat de polymère amorphe. La phase solide a donc la même structure cristalline sur l'eau et sur substrat solide. Les intensités relatives des pics sont comparables dans les deux expériences, ainsi que dans le modèle proposé pour la structure moléculaire. Ce modèle rend également compte de l'anisotropie très importante de la phase cristalline et de ses propriétés optiques. Il pourrait s'agir d'une phase ferroélectrique, comme cela avait été précédemment supposé pour expliquer la forme allongée des cristaux.

Abstract. — Grazing incidence X-ray diffraction is performed on a Langmuir monolayer made of pure fluorescent NBD-stearic acid, spread at the free surface of water. It shows several intense narrow peaks in the solid phase, at the same wavevectors as the brightest peaks observed earlier by electron diffraction, for a monolayer transferred onto an amorphous polymer substrate. Thus the solid phase has the same crystalline structure on water and on solid substrate. The relative peak intensities are comparable in both experiments, and in the proposed model for the molecular structure. This model also accounts for the very large anisotropy of the crystalline phase and its optical properties. This phase could be ferroelectric, as previously assumed in order to explain the elongated shape of the crystals.

(*) Also at Institut für Physikalische Chemie, Universität Mainz, Jakob Welder Weg 11, D6500 Mainz, Germany.

(**) Associé au CNRS et aux Universités Paris VI et Paris VII.

Introduction.

NBD-stearic acid is a fluorescent fatty acid which can be easily spread on water as a single component insoluble monolayer [1]. The nitrobenzoxadiazole (NBD) dye is attached on the twelfth carbon (Fig. 1a), and allows to visualize the monolayer with an optical microscope. A plateau in the two-dimensional (2D) isotherm indicates that a first-order transition occurs in the monolayer at a surface pressure $\Pi = 8$ mN/m ($T = 20$ °C), between a fluid phase (area per molecule $A_f \approx 84$ Å²) and a denser one ($A_s \approx 32$ Å²) (Fig. 1b). Direct observations on the plateau show bright elongated domains, with needle shapes, coexisting with the dark fluid phase (Fig. 2). At rest, their size and aspect ratio vary with earlier growth conditions. Typically, the width is 10 to 50 μm, and the length a few hundred micrometers, up to several millimeters when growth is very slow.

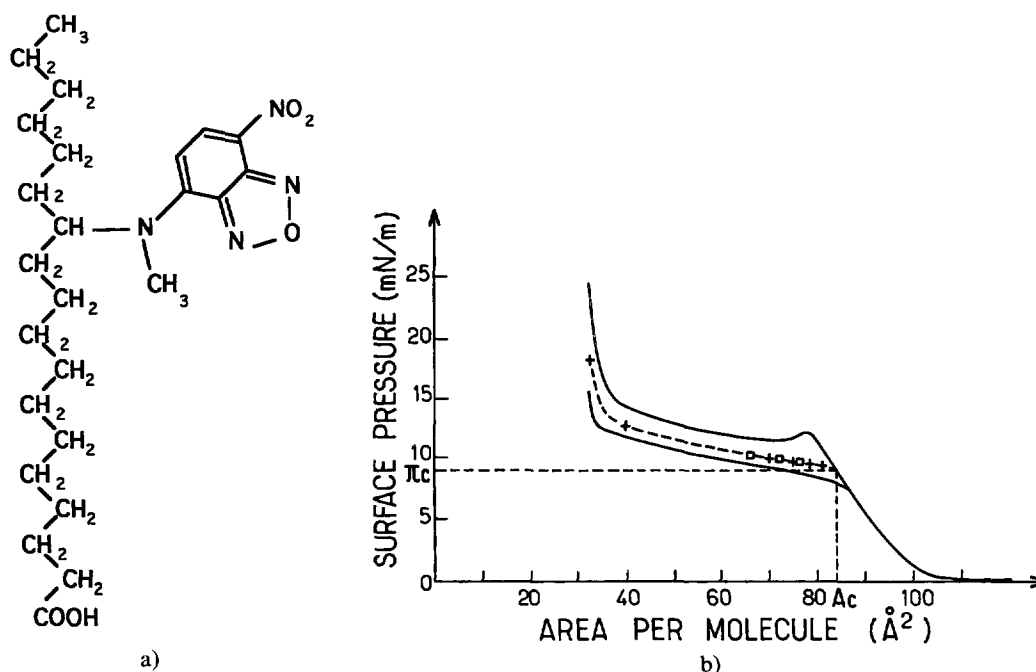


Fig. 1. — Structure of the NBD-stearic acid molecule and surface isotherm for a monolayer at $T = 20$ °C, on acidified water (pH = 2) (from Ref. [1]); full line : compression and decompression (compression rate 2 Å²/mol/mn) ; dashed line : equilibrium isotherm.

An important question is whether this phase is a 2D crystal, with long-range positional order of the molecules (or at least quasi-long range positional order, as no true crystal exists in two dimensions [2]). It is already known that the domains are 2D solids : they can be elastically bent before breaking, and their 2D Young's modulus has been measured [3, 4]. Macroscopic evidence for order in this solid phase comes from optical anisotropy : the needle absorption dipole is maximum along its small axis, meaning that the molecular transition dipoles are ordered in the domains. Moreover, broken needles exhibit a fibered substructure parallel to their long axis, on a scale of the order of optical resolution (≤ 1 μm). The same fibers are visible when a needle is illuminated by a high intensity light beam at the maximum absorption wavelength ($\lambda_{\text{abs}} = 480$ nm), causing fluorescence bleaching and partial melting of the needle.



Fig. 2. — Photograph of a NBD-stearic monolayer at the first order solid/liquid phase transition : bright 2D crystals (needles) coexist with the liquid phase. This phase appears to be dark probably because the chains lie on water and the fluorescence of the NBD probes in contact with water is quenched. The bar length is 200 μm .

Electron diffraction provides evidence for a crystalline phase, since the diffraction pattern of a monolayer in the solid state, transferred onto an amorphous polymer substrate (formvar) presents several well-defined narrow peaks, up to high orders [5]. It was thus important to perform a grazing incidence X-ray diffraction experiment at the air-water interface, to decide whether the transfer could have modified the molecular structure. We show that no such modification occurs, since X-ray scattering from the solid phase gives four intense peaks at the same position as the brightest electron peaks. We compare the peak wavevectors and intensities in X-ray and electron experiments, and conclude that the molecular structure is the same on water and on solid substrate.

We propose a model for the lattice. The unit cell is rectangular and contains eight molecules. The hydrophobic chains partially fill a triangular lattice, and are packed together along parallel stripes. The NBD planes are vertical and set up in a herringbone structure. This arrangement explains the main properties observed on the macroscopic scale (morphological and optical anisotropy). One of the open questions which motivated this work was the possible ferroelectricity of the solid phase, suggested in an earlier model to explain the elongated needle shape [6]. We discuss the existence of a finite dipolar density on the proposed structure.

Experimental set-up and results.

Grazing incidence X-ray diffraction was carried out on the D24 beam line of the Dispositif de Collisions sous Igloo (DCI), in the Laboratoire pour l'Utilisation du Rayonnement Electroma-

gnétique, LURE, at Orsay (France). The beam is in the horizontal plane, and is made monochromatic ($\lambda = 1.49 \text{ \AA}$) on the (111) vertical face of a Ge crystal, with asymmetrical cut and slight curvature for focussing. Its divergence is 1 mrad. A silica mirror is used to deflect the beam slightly down onto the water surface. The incidence angle is 1.42 mrad, below the critical angle for total external reflection. Between the mirror and the trough, the beam is collimated through Huber slits (100 μm high and 5 mm wide). The incident intensity is monitored by a ionization chamber. To reduce parasitic scattering the beam is conducted through evacuated or helium filled tubes whenever possible. Scattered X-rays are counted by a 5 cm wide NaI scintillation detector, rotating azimuthally around the sample. Sollers slits are used for horizontal collimation, their full angle acceptance is 2.6 mrad. The theoretical resolution in transfer wavevector q is of the order of 0.01 \AA^{-1} (Full Width at Half Maximum : FWHM). Due to the height of Sollers slits, the integration range along the vertical direction is $0 < q_z < 0.3 \text{ \AA}^{-1}$. The area of the teflon home-made Langmuir trough ($460 \times 120 \times 4 \text{ mm}^3$) varies from 500 to 140 cm^2 by means of a teflon piston. The surface pressure is measured with a filter paper Wilhelmy plate. The trough is enclosed in a plexiglas cover, in which two kapton windows (25 μm thick) allow the passage of the X-ray beam. The trough parameters are monitored from outside by a computer. Experiments are carried at room temperature. NBD-stearic acid (purchased from Molecular Probes) is used without specific purification and is spread on acidified (pH = 2) water from a solution in chloroform ($\sim 0.01 \text{ M}$). During diffraction experiments, the surface pressure is regulated at $\Pi = 15 \text{ mN/m}$, in the solid phase region. Optical observations have shown that, at this pressure, around 90 % of the surface is covered by needles having random orientations, and 10 % by the liquid phase trapped between the needles. Because of the typical needle size ($\sim 100 \mu\text{m}$), the film has to be considered as a powder.

Several runs have been performed for different sets of q vectors, ranging from 0.3 to 1.6 \AA^{-1} . Figure 3 shows the bare scattered intensity as a function of q , different runs being superimposed. Over a continuous decrease of the intensity, four different peaks appear. In figures 4a-d, the interesting areas are enlarged. Following the procedure described in

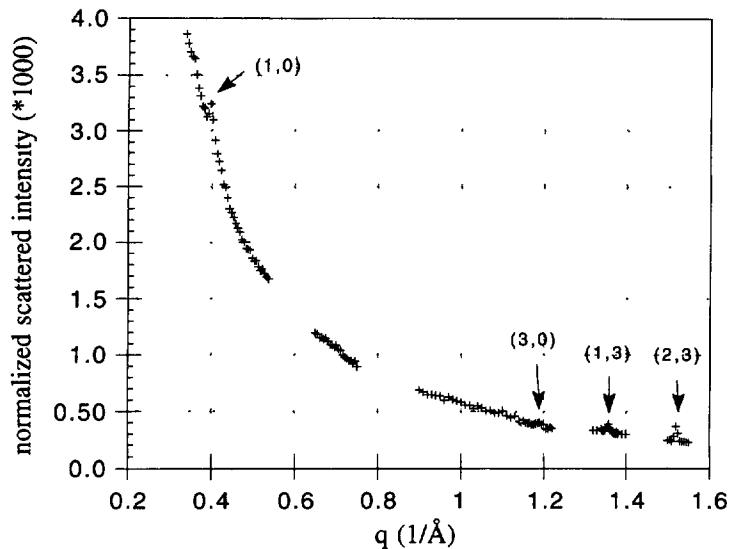


Fig. 3. — Plot of the X-ray scattered intensity *versus* momentum transfer q . The intensity is normalized to the incident beam intensity. The arrows indicate the detected peaks.

reference [7], the bare intensity has been multiplied by $\tan^2(2\theta)$, to account for the beam cross section area correction $\sin(2\theta)$, the Lorentz factor $\sin(2\theta)$ and the polarization factor $1/\cos^2(2\theta)$. The best Gaussian fits on a sloping background, obtained with a maximum entropy algorithm (ABFfit program), are also represented. The exact respective peak positions (and FWHM) are, in \AA^{-1} : 0.398 (0.013); 1.190 (0.016); 1.358 (0.009); 1.521 (0.009) (see also Tab. I). Notice that the width is comparable to the instrumental resolution. An extra $1/\cos(\theta)$ must be applied to calculate the integrated intensity in each peak, because the runs were performed by steps of constant Δq and not constant $\Delta\theta$.

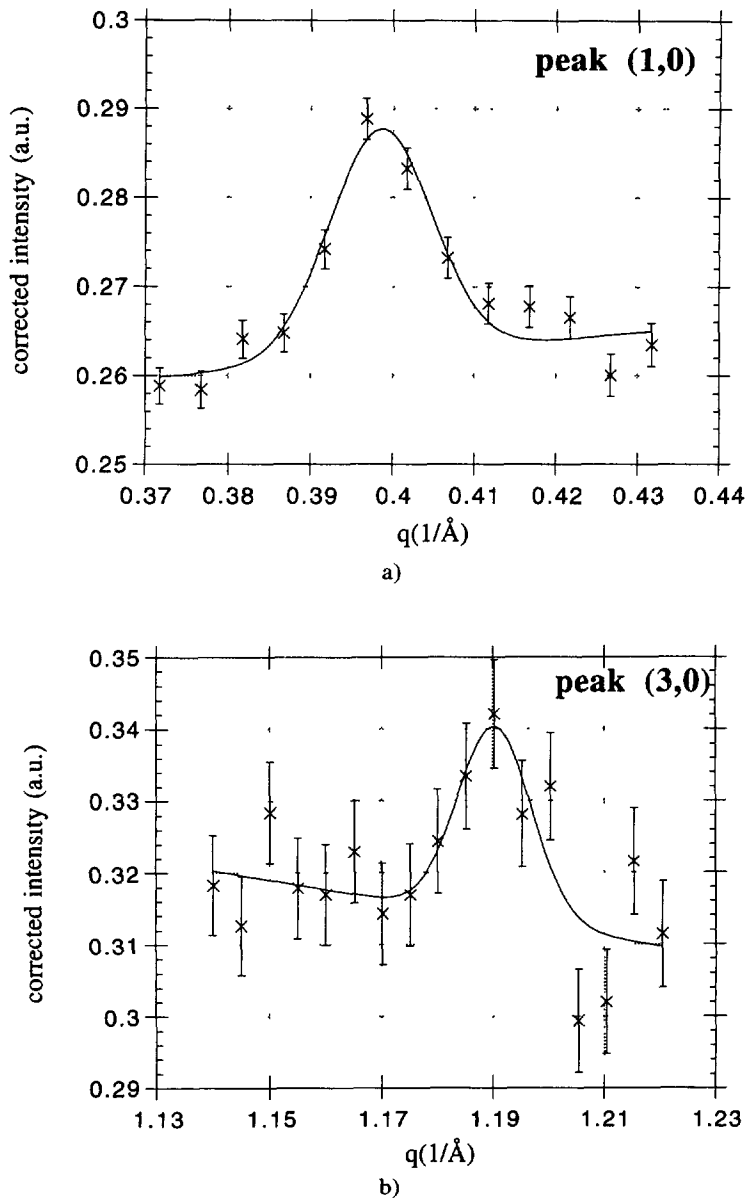
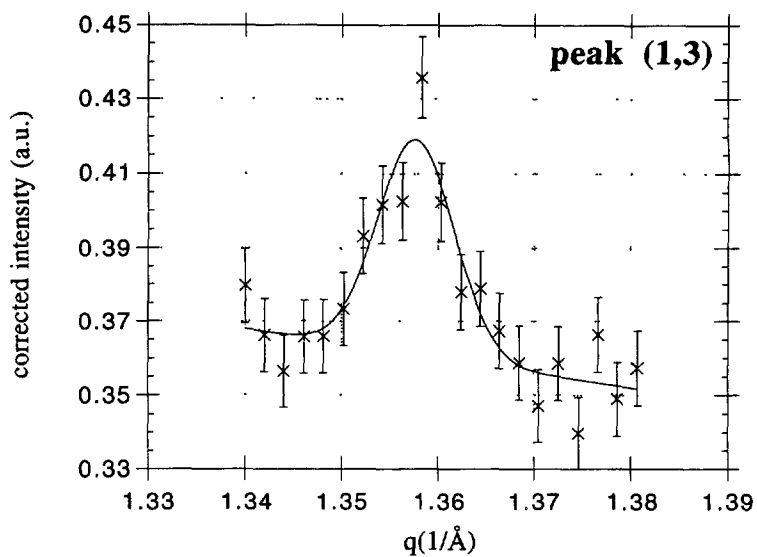
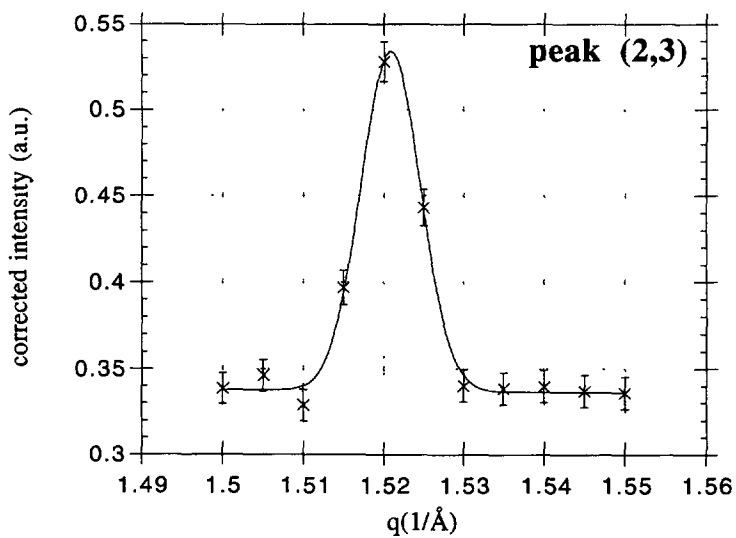


Fig. 4. — a to d: Enlarged view of the four detected peaks. The intensity has been corrected by geometrical factors (see text). The best Gaussian fits are also shown.



c)



d)

Fig. 4 (continued).

Table I.

peak indices	q vector (\AA^{-1}) (electrons)	q vector (\AA^{-1}) (X ray)	relative intensity (electrons)	relative intensity (X ray)	relative calculated intensity
(1,0)	0.40	0.398	0.18	0.41	0.43
(2,0)	-	-	0	0	0.07
(3,0)	1.19	1.190	0.45	0.43	0.39
(1,3)	1.365	1.358	0.51	0.34	0.32
(2,3)	1.52	1.521	1	1	1
(4,0)	1.59	-	0.52	-	0.45

Comparison with electron diffraction.

Earlier electron diffraction experiments were performed on a NBD-stearic film transferred onto an amorphous polymeric substrate (formvar) [5]. Since the electron beam is about $1\ \mu\text{m}$ wide, it illuminates a single needle. The electron diffractogram is shown in figure 5. Many narrow peaks are visible, up to high orders, forming a rather complicated pattern. At least on formvar, this phase is a 2D crystal, with long-range correlations of the molecular positions. The lattice is rectangular, and the size of the elementary cell is $15.8 (\pm 0.5) \times 14.5 (\pm 0.5)\ \text{\AA}^2$. In the following, the peaks will be labelled by Miller indices (h, k) . Several important features appear on the diffractogram : first the $(0, 3)$ and $(2, 0)$ peaks appear extinguished. Secondly, the brightest peaks are $(3, 0)$, $(4, 0)$, $(2, 3)$, $(1, 3)$ and symmetrical positions. They are

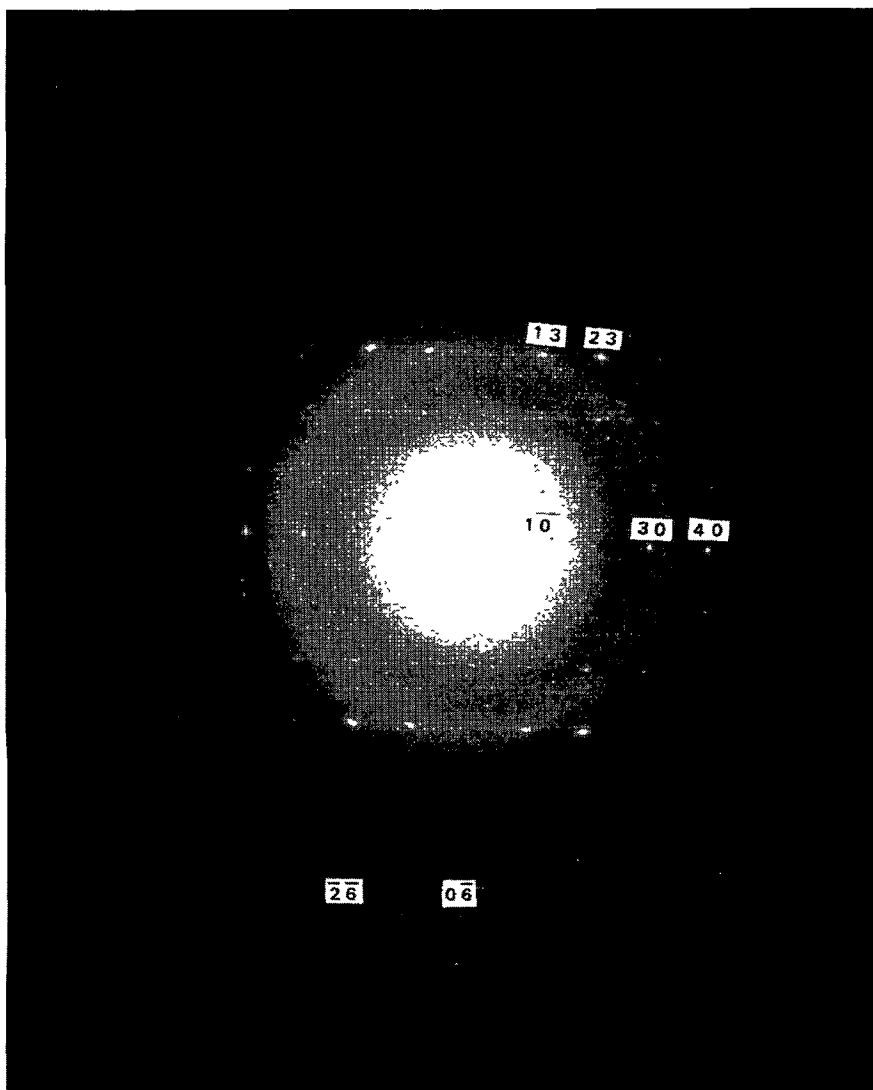


Fig. 5. — Electron diffractogram from a needle (solid phase) transferred onto a formvar substrate. The main peaks of the rectangular lattice are labelled by Miller indices (h, k) .

organized on a roughly hexagonal pattern. The (1, 0) peak is also a bright one, although it is hardly visible on the photograph shown because of the direct beam. Several secondary peaks are visible, especially (0, 6), (1, 6), (2, 6) and symmetrical positions, and a series of diffuse peaks on the $k = \pm 2$ rows. This diffraction pattern does not correspond to any simple structure, and the molecular arrangement in the unit cell should be complex.

In table I are reported together the four wavevectors of X-ray peaks and the five wavevectors of the brightest electron peaks. Within experimental errors, the peak positions are exactly identical in both cases. The $q = 1.59 \text{ \AA}^{-1}$ peak is unfortunately missing in X-ray data, because we did not explore carefully this q region. The comparison between the integrated peak intensities in both experiments is also presented in table I. The X-ray relative integrated intensities are calculated from the fits for the peaks. The intensity of the brightest (2, 3) peak ($q = 1.521 \text{ \AA}^{-1}$) is set up to 1 as a reference. The electron intensities are measured from the optical density D of the negative photographic film, supposing that D is proportional to the exposure [8]. Again the brightest (2, 3) peak intensity is set up to 1. The intensity ratios are comparable. One does not expect a better agreement, since the substrate is different in both experiments, and the diffraction technique too : X-ray diffraction is sensitive to the electron density, while electron diffraction is sensitive to the electrostatic potential.

The conclusion is that the solid phase in a NBD-stearic acid monolayer on water is a 2D crystal, which molecular structure is not affected by the transfer onto the amorphous substrate. From X-ray experiments, the largest peak width gives a typical value for the correlation length in the crystal of the order of 400 \AA . It was not possible to measure this length from electron diffraction data.

A model for the molecular structure.

The unit cell area, determined by X-ray diffraction, is $15.8 \times 14.5 = 229 \text{ \AA}^2$ ($\pm 0.1 \text{ \AA}$ on each dimension). On the other side, the average area per molecule determined from the isotherm at $\Pi = 15 \text{ mN/m}$ is about 32 \AA^2 . At this pressure, the solid phase occupies roughly 90 % of the surface, thus one calculates that the area per molecule in this phase is approximately $A_{st} = 30 \text{ \AA}^2$. The unit cell contains several molecules, and the two possibilities are :

i) 7 molecules per cell. Then the area per molecule is $A_s = 32.7 \text{ \AA}^2$. This is slightly too large to be consistent with A_{st} , since, because of possible defects in the structure, one expects A_s to be smaller than A_{st} . Moreover, a cell containing an odd number of molecules seems very unlikely. In our case, the carbon labelled by the NBD group is asymmetric, but the sample is racemic. Thus, the only way to get seven molecules per cell would be homochiral discrimination of the molecules, leading to right and left crystals. Because we never observed any manifestation of chirality on the needle macroscopic properties, neither during growth nor at equilibrium, we discard this possibility.

ii) 8 molecules per cell and $A_s = 28.6 \text{ \AA}^2$. This is fully consistent with A_{st} , and we keep this number of molecules in the following discussion.

In a first step, we need to know the molecular configuration perpendicular to the layer. X-ray reflectivity experiments have been done on a monolayer transferred onto a silicon wafer [9]. A very good fit to the data is obtained for a monolayer thickness $d = 25.1 \text{ \AA}$, and for the NBD dye located at a height corresponding to the twelfth carbon. This indicates that, at least on silicon, the hydrophobic chain is straight and vertical in the dense phase. The smallest area per molecule in a pure fatty acid solid phase (triangular lattice) is 19 \AA^2 , corresponding to 17 \AA^2 for the molecule itself, modelled as a disk. The estimated size of the NBD plane is $6 \times 5.5 \text{ \AA}^2$ in its plane and $6 \times 2.5 \text{ \AA}^2$ from a side view. To achieve an area per molecule of 28 \AA^2 , the NBD planes have to be set up vertically, partially overlapping, and the molecular

packing must be very tight. We believe that, due to this high packing, the crystal cohesion energy is very large, and that the molecular configuration should not depend very much on the interactions with the substrate, either silicon, formvar, or water.

We adopt for the molecule the schematic representation shown in figure 6a. From a top view, the chain and polar head are sketched as a dark circle (4 Å in diameter). The NBD plane is drawn as a grey $5 \times 2 \text{ \AA}^2$ rectangle linked to the chain in a non-symmetric way, to respect the molecular chirality. The two different grey levels have been chosen to roughly represent the electron density in the molecule (159 electrons in the chain, 99 in the dye). The crystal structure is then modelled as follows : a two-dimensional molecular array is drawn, containing 12×12 elementary cells, and its Fast Fourier Transform (FFT) is compared to the diffraction data (peak positions and intensities). A Gaussian mask is applied over the sides of the array to avoid parasitic streaking on the FFT.

The electron diffraction pattern exhibits a pseudo-hexagonal symmetry with intense peaks at $q \approx 1.5 \text{ \AA}^{-1}$. This is the signature of an underlying triangular lattice for the chains. From the diffractogram, one sees that there should be 4×3 sites of this triangular lattice in the unit rectangular cell. Figure 6b shows a model for this elementary cell, in which the NBD groups have not been represented. The spacing of the triangular sublattice is 4.8 Å in the y direction, slightly squeezed in the x direction. This is identical to the spacing in the dense phases of common fatty acids. In the real cell, only 8 sites out of 12 have to be occupied by a molecule. This leads to a finite number of combinations, and we recover the main features of the diffractogram only when the chains are packed together in stripes parallel to the y axis, leaving empty alleys between them. The FFT of the corresponding array is similar to the experimental patterns : the (1, 0), (3, 0), (4, 0), (1, 3) and (2, 3) peaks are the brightest, while (2, 0) and (0, 3) are extinguished. However, the relative peak intensities are different from the measured ones, sometimes by more than one order of magnitude. A better result is obtained when adding the NBD planes, setting them in the empty space between the chains. We have determined by an independent optical method the angle α between the NBD plane direction

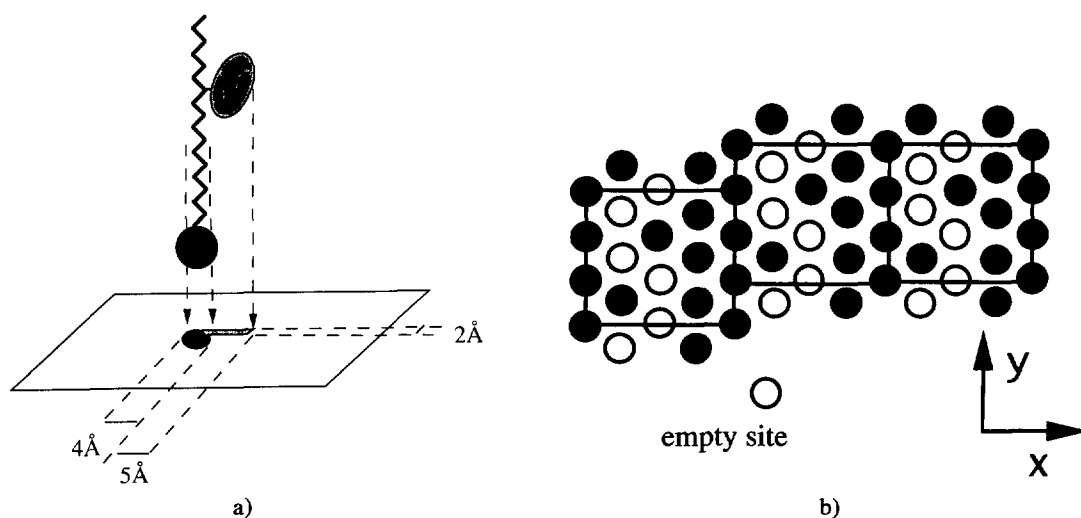


Fig. 6. — a) Schematic representation of the NBD-stearic acid molecule in a top view projection, used for the structure simulations ; b) sketch of the elementary cell : 8 molecules are distributed on the 12 sites of a triangular lattice. Only the aliphatic chains are represented, not the NBD dyes. Random slipping of the cells by $1/3$ of the lattice spacing is allowed in the y direction.

and the x axis. This method, based on reflectivity measurements under polarized light in the absorption band, will be described elsewhere [12]. We found $\alpha \approx \pm 25^\circ$. There are several ways to achieve this packing, by setting the NBD planes either parallel or in a herringbone structure inside the same stripe. Parallel NBD planes correspond to $\alpha = +25^\circ$, or -25° , in each stripe, alternatively. This would lead to additional peaks in the $k = 3$ and $k = 6$ rows, which are not seen on the diffractogram. The closest agreement with the experimental data can be achieved with the herringbone structure. It is shown in figure 7a, and the corresponding FFT in figure 7b. One recovers most of the details of the diffraction data, including the $k = 6$ row. Moreover, the $k = 2$ row of diffuse peaks, visible on the electron diffractogram, is simulated by allowing a random translation ($\pm 1/3$ of the lattice spacing) of the chain stripes in the y direction, as shown in figure 6b. This is physically reasonable, since the cohesion between adjacent stripes is piloted by van der Waals chain-chain interactions, weaker than in the perpendicular direction, where dipole-dipole interactions dominate.

The peak intensities are calculated from the FFT power spectrum. They are reported in table I, to be compared with the measured ones. Simulation and X-ray intensities agree within 10 %, which is quite good, considering the oversimplified representation we took for the molecule. The comparison with electron intensities is not so good. This is not surprising, as electrons are sensitive to the potential while X-rays are sensitive to the electron density. One notices that the $(2, 0)$ calculated intensity is not exactly zero. Actually, this peak has no peculiar reason to be exactly extinguished, since the $(4, 0)$ peak is bright. Also, dumping the high order peaks by adding a 2D Debye-Waller factor does not change significantly the agreement. Finally, we have simulated slight variations of the lattice parameters (molecular size, spacing, positions, and orientation α): we observe significant changes in the pattern and in the calculated intensities when the two main characteristics of the lattice are modified, i.e. the organization of the chains in parallel stripes and the herringbone arrangement of NBD planes. Thus we believe that the structure determined by this method is reasonably close to the real structure, all the more as it explains most of the macroscopic properties of the solid phase, as discussed in the next section.

Relation to macroscopic properties.

In the above description, the large needle anisotropy is directly related to the molecular structure. It is natural to believe that the needle axis is parallel to the stripes defined by the aliphatic chains (y axis). This hypothesis is supported by several arguments. First, a fibered structure is visible in the needles, either when they break, or when they are melted under intense lightening. This is consistent with a weak coupling and easy slipping between parallel stripes. Second, it has been shown that light absorption is maximum in the direction perpendicular to the needle axis. According to models, the molecular absorption dipole is in the NBD plane [10]. Then the absorption momentum in figure 7 has its maximum along the expected orientation, perpendicular to the stripes.

One of the issues of this structural determination was the possible existence of a permanent in-plane macroscopic dipole. Besides the transition dipole, the NBD dye also has a permanent dipole moment in its plane, oriented towards the aliphatic chain [6]. In figure 7, each stripe carries a resultant dipole finite and parallel to it, resulting in an average 2D dipole density in the y direction. This is consistent with the main hypothesis used to model the needle shape [6]. However, this should not be considered as an unambiguous evidence for 2D ferroelectricity. An antiferroelectric state can be easily simulated by applying a $y \rightarrow -y$ symmetry to half the stripes. Then, the calculated diffraction pattern looks slightly different, new peaks appearing in the $k = 3$ row. However, their intensity is small and may not be experimentally measurable. Although we believe that the needle structure is more likely ferroelectric than antiferroelectric,

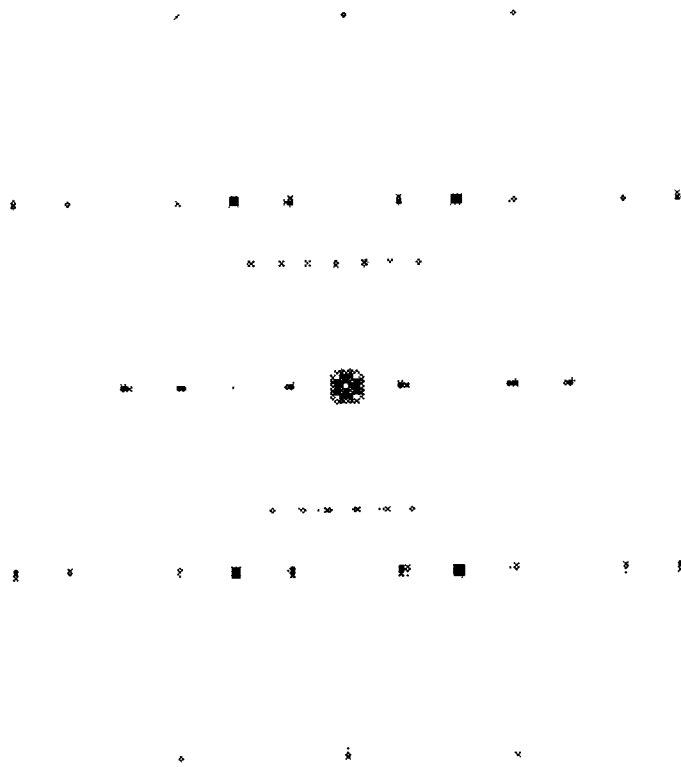
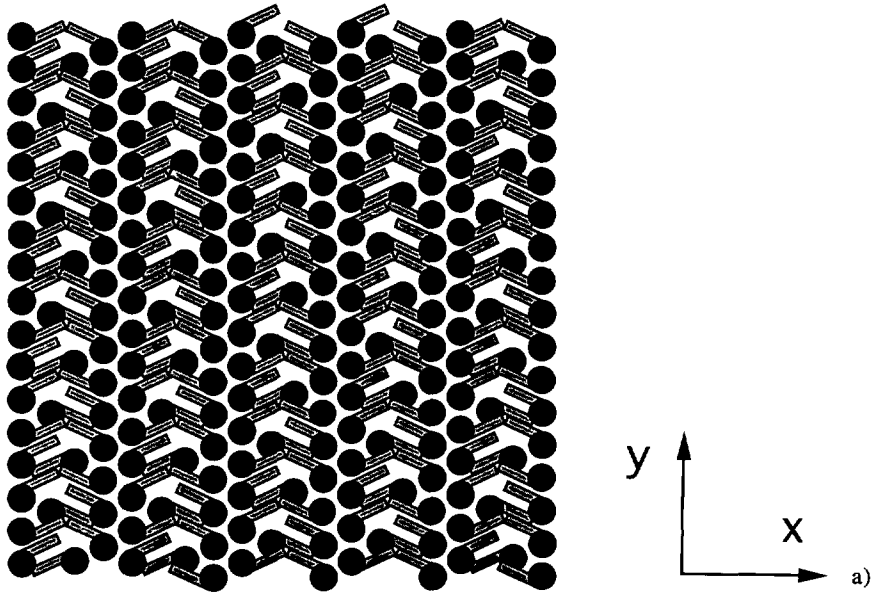


Fig. 7. — a) Complete simulated molecular structure giving the best agreement with the diffraction data ; b) its Fast Fourier Transform (power spectrum).

a definite conclusion should come from any other direct experimental evidence. First, one can think about orienting the needles in an external electric field. Unfortunately this experiment cannot be performed, since the underlying water is a conducting substrate : any horizontal field would be screened on the Debye-Hückel length, which is always smaller than the needle size (at most 1 μm for pure water). Another possibility is to make a second harmonic generation (SHG) experiment : a signal should be seen only if the structure is not centrosymmetric. As a preliminary result, SHG has recently been detected from a NBD stearic acid monolayer on water [11]. This gives additional confidence in the molecular interpretation presented in this paper.

To summarize and to conclude, the diffraction data definitely show that in a monolayer made of fluorescent NBD-stearic acid spread on water, the solid phase is a 2D crystal with long-range positional order. Comparison between diffraction on water and on an amorphous solid substrate show that the molecular structure is the same in both cases. A model for this structure is presented, in quantitative agreement with experiments, and accounting for the macroscopic physical properties of this crystalline phase. At this stage, we have good theoretical and experimental indications that this crystalline phase is a 2D ferroelectric. We expect that a confirmation of this property will be brought in a near future by other direct experimental evidence.

Acknowledgements.

We acknowledge P. Nassoy and R. Kenn for their active participation to the LURE experiment, C. Bourgaux and P. Vachette and the staff of LURE for beam time. Thanks also to A. Schalchli and J. J. Benattar who made X-ray reflectivity experiments on our samples.

References

- [1] Bercegol H., Gallet F., Langevin D. and Meunier J., *J Phys. France* **50** (1989) 2277.
- [2] Peirls R. E., *Ann. Inst. H. Poincaré* **5** (1935) 177.
- [3] Bercegol H. and Meunier J., *Nature* **356** (1992) 226.
- [4] Pauchard L. and Meunier J., *Phys Rev. Lett.* **70** (1993) 23.
- [5] Flament C., Graf K., Gallet F. and Riegler H., Proceedings of LB 6 Conference (Trois Rivières, Québec, July 93), to appear in *Thin Solid Films*.
- [6] Muller P. and Gallet F., *J. Phys. Chem.* **95** (1991) 3257.
- [7] Kjaer K., Als-Nielsen J., Helm C. A., Laxhuber L. A. and Möhwald H., *Phys. Rev. Lett.* **58** (1987) 2224 ;
Leveiller F., Jacquemain D., Leiserowitz L., Kjaer K. and Als-Nielsen J., *J. Phys. Chem* **96** (1992) 10380 ;
Dutta P. and Sinha S. K., *Phys. Rev. Lett.* **47** (1981) 50.
- [8] Kirstein S., PhD thesis, Mainz University (1992) (unpublished).
- [9] Benattar J. J. and Schalchli A., unpublished results.
- [10] Mori J. and Kaino T., *Phys. Lett. A* **127** (1988) 259.
- [11] Kunz S. and Muller P., private communication.
- [12] Flament C. and Gallet F., to be published. In a previous paper [5], we wrote $\alpha = 15^\circ$. We now believe that this independent determination $\alpha = 25^\circ$ is more accurate.